



Synthesis of Styrofoam Waste-Derived Activated Carbon as an Electron Extractor for Modifying Cu/P-CuSCN/N-Cu₂O/ITO Photovoltaic Cells

Dheani Laily¹, Aisyah Wahyu Fitriani¹, Endar Aldi Hanantya¹, Rahmad Nuryanto^{1,*}



¹ Chemistry Department, Faculty of Sciences and Mathematics, Diponegoro University, Jl. Prof. Soedarto, SH., Tembalang, Semarang, Indonesia

* Corresponding author: nuryantorahmad@live.undip.ac.id

<https://doi.org/10.14710/jksa.27.10.485-490>

Article Info

Article history:

Received: 04th July 2024
 Revised: 17th October 2024
 Accepted: 28th October 2024
 Online: 30th October 2024

Keywords:

Activated carbon; Photovoltaic;
 Styrofoam waste; Electron
 extractor

Abstract

Activated carbon synthesized from styrofoam waste was applied as an electron extractor to enhance the performance of Cu/p-CuSCN/n-Cu₂O/ITO-based photovoltaic cells. The widespread use of plastic products, particularly styrofoam, has led to severe environmental pollution due to its long decomposition time. Styrofoam waste-derived activated carbon utilizes polystyrene, which is rich in carbon, to produce high-surface-area materials. In this study, the activated carbon enhances the efficiency of photogenerated electron separation and extraction in photovoltaic cells. Characterization results indicate that the activated carbon has a surface area of 1,865.04 m²/g, a pore volume of 1.25 cm³/g, and a pore diameter of 2.53–2.68 nm, with a direct band gap energy of 4.33 eV. Voltage testing on the photovoltaic cells demonstrated a significant increase, with the highest voltage reaching 209.67 mV in the 5 mg activated carbon variation, representing a 34.84% improvement. The application of activated carbon in Cu/p-CuSCN/n-Cu₂O/ITO-based photovoltaic cells provided a notable voltage increase, confirming its effectiveness as an electron extractor.

1. Introduction

The use of plastic products increases each year. Excessive production of plastic packaging, coupled with inadequate waste processing, leads to environmental pollution. In 2016, Indonesia ranked fifth in global plastic waste production, generating 9.128 million tons of plastic waste [1]. One major type of plastic waste is styrofoam, which decomposes much more slowly than other plastics, typically taking between 60 and 1,000 years [2]. Styrofoam is often disposed of by incineration, which contributes to environmental pollution through emissions of CO₂, SO_x, and chlorine gas [1]. The main component of styrofoam, polystyrene, consists of a long carbon chain formed from repeating styrene monomers (C₈H₈) [3]. Rich in carbon groups, styrene monomers offer the potential for conversion into activated carbon, which features a large surface area, ample porosity, and high adsorption capacity [4]. Activated carbon is valuable across various fields, including technology, industry, and energy.

According to data from the Central Statistics Agency (BPS) for 2019–2021, the most widely installed power plants in Indonesia are Steam Power Plants (PLTU), with 33,092 units. Coal-fired PLTUs emit CO₂ at a rate of 1,140 tons per MWh [5]. To address this, the Presidential Regulation of the Republic of Indonesia Number 112 of 2022 on Accelerating Renewable Energy Development for Electricity Supply promotes alternative energy sources, including Solar Power Plants (PLTS), to reduce the burden on PLTUs. In this context, photovoltaic cell performance can be enhanced by utilizing activated carbon as an electron extractor, which facilitates the separation and extraction of photogenerated electrons, thereby reducing recombination losses [6]. Activated carbon can serve as an electron extractor due to its semiconductor properties [7] and a band gap range of 0–5 eV [8]. Yuningsih and Mulyadi [9] reported that activated carbon from coconut shells achieved a conductivity of 0.8 S/cm, while corn cob-derived activated carbon reached 0.7 S/cm [7].

Previous studies have studied various electron extractor materials for photovoltaic cells, including graphene oxide (GO) [10]. However, the relatively low surface area of GO limits its effectiveness in electron collection and extraction, reducing the overall efficiency of photovoltaic cells. In contrast, activated carbon offers a much larger surface area—typically between 500 and 1,500 m²/g for commercial activated carbon, compared to 150 m²/g for commercial GO [11, 12]. As an electron extractor, activated carbon provides more reactive sites on its surface, enhancing charge transfer efficiency from the active layer to the electrode. Additionally, its porous structure enables faster electron diffusion, making it a superior material for electron collection and transport in photovoltaic energy storage and conversion applications.

The issues outlined above serve as the backdrop for the innovative development of Cu/p-CuSCN/n-Cu₂O/ITO-based photovoltaic cells, utilizing activated carbon derived from styrofoam waste as an electron extractor. The Cu/p-CuSCN/n-Cu₂O/ITO structure [13] has demonstrated good stability and efficiency; however, modification with activated carbon from styrofoam waste presents a more optimal solution due to its surface area characteristics, enhancing photovoltaic cell performance. This innovation not only boosts the efficiency of photovoltaic cells but also addresses environmental challenges, such as air pollution and styrofoam waste while providing an alternative renewable energy source.

2. Experimental

2.1. Tools and Materials

Various tools and instruments were used, including glassware, sandpaper, filter paper, dropper pipettes, measuring cylinders, flasks, and pipettes, as well as stirring rods, water baths, hot air guns, vertical and horizontal furnaces, pH meters, micrometers, voltmeters, crucibles, ovens, spatulas, Brunauer-Emmett-Teller (BET) apparatus, and UV-Vis Diffuse Reflectance Spectroscopy (DRS). The materials used include styrofoam waste, 100% acetone (True Glitter), anhydrous KOH, 10% HCl (Mallinckrodt), copper plate, KSCN (Merck), 100% CH₃COOH (CIMS), 1 M CuSO₄ (Sains Laboratory), ITO glass (10 ohms), and nitrogen gas.

2.2. Synthesis of Activated Carbon from Styrofoam Waste

Activated carbon was synthesized using a method adapted from de Paula *et al.* [14] with modifications to the inert gas used. The process began by dissolving styrofoam waste in acetone, followed by drying with a hot air gun. The dried sample was then placed in a vertical furnace, heated to 530°C at an average rate of 10°C/min under N₂ gas for 5 hours. Activation was performed using anhydrous KOH as the activating agent, with a KOH to pyrolyzed styrofoam waste ratio of 4:1. The mixture was then heated in the furnace at 800°C for 1 hour. Finally, the activated carbon was washed with 10% HCl and rinsed with hot distilled water until a pH of 7 was achieved.

2.3. Preparation of Cu/p-CuSCN/n-Cu₂O/Activated Carbon/ITO

The copper plate was first sanded with sandpaper, and its thickness was measured. It was then washed with distilled water, cleaned using an ultrasonic device, and soaked in a solution containing 0.1 M KSCN, 0.1 M acetic acid, and 1 M acetone, adjusted to a pH of 3.5, for 30 minutes to form a p-CuSCN layer (positive semiconductor). The negative semiconductor was obtained by boiling the Cu/p-CuSCN plate in a 1 M CuSO₄ solution for 30 minutes, resulting in the formation of an n-Cu₂O layer on top of the plate. Activated carbon from styrofoam waste was then deposited on the Cu/p-CuSCN/n-Cu₂O plate with varying weights of 0, 1, 2, 3, 4, and 5 mg. Finally, ITO glass was added to complete the assembly of the photovoltaic cell [15].

3. Results and Discussion

3.1. Synthesis of Activated Carbon from Styrofoam Waste

Figure 1 shows the results of activated carbon, which appears as fine black grains and has a neutral pH, as confirmed by pH indicator testing. The flow of N₂ gas prevents oxidation by reducing the oxygen content during the pyrolysis process in the furnace [16]. A temperature of 530°C is considered optimal for the styrofoam pyrolysis process, as pyrolysis temperatures generally range from 400°C to 650°C [17]. The pyrolyzed carbon was then activated using KOH, which significantly affects the structure and porosity of the activated carbon [17]. The styrofoam waste-derived activated carbon was characterized using the BET method and UV-Vis DRS.

3.1.1. Brunauer-Emmett-Teller (BET) Characterization

The pore size characteristics of the styrofoam waste-derived activated carbon were analyzed using the BET method, which is based on the gas absorption capacity. Nitrogen gas was used for the characterization. The resulting linear isotherm graph, shown in Figure 2, illustrates the nitrogen gas absorption capacity of the activated carbon sample. The graph corresponds to a Type IV isotherm, indicating that the activated carbon is mesoporous, with pore sizes ranging from 2 to 50 nm [18]. The detailed results of the BET characterization for the styrofoam waste-derived activated carbon are presented in Table 1.



Figure 1. Activated carbon derived from styrofoam waste

Table 1. BET surface area and pore volume

Sample	BET surface area (m ² g ⁻¹)	Pore volume (cm ³ g ⁻¹)	Pore diameter (nm)
Styrofoam waste-derived activated carbon	1,865.04	1.25	2.53-2.68

Based on Table 1, the surface area of the styrofoam waste-derived activated carbon was 1,865.04 m²/g, with a pore volume of 1.25 cm³/g and a pore diameter ranging from 2.53 to 2.68 nm. The surface area of this activated carbon is larger compared to that of polyacrylonitrile-based activated carbon (1,250 m²/g) [19] and polyurethane foam-derived activated carbon (1,469.9 m²/g) [20]. The pore diameter of 2.53–2.68 nm falls within the mesoporous range (2–50 nm), which is advantageous for maximizing light absorption across various wavelengths and preventing the diffusion of captured electrons [21]. The BET characterization results demonstrate that styrofoam waste-derived activated carbon is suitable as an electron extractor in Cu/p-CuSCN/n-Cu₂O/ITO-based photovoltaic cells.

3.1.2. UV-Vis DRS (Diffuse Reflectance Spectroscopy) Analysis

Styrofoam waste-derived activated carbon samples were tested using UV-Vis DRS in the wavelength range of 100–400 nm. The resulting data were used to calculate the band gap energy (E_g), which is presented in Figure 3. The band gap energy was determined using the Kubelka-Munk equation and the Tauc plot method, where E_g is derived from the graph of the relationship between (F(R'[∞])/hv)ⁿ and hv (eV) [22]. The band gap energy corresponding to direct electron transitions is shown in Figure 3, where the value of n is 2 [23].

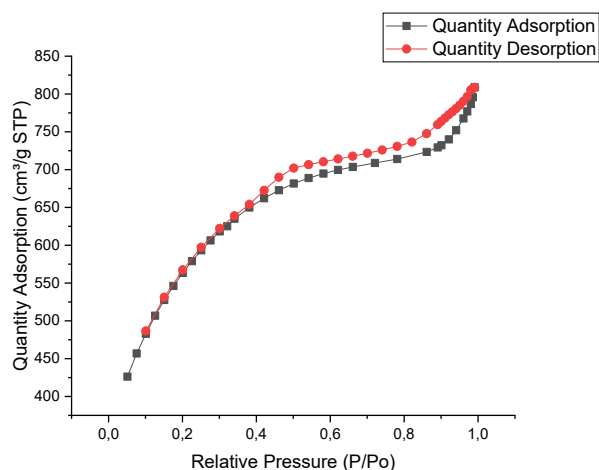


Figure 2. BET adsorption and desorption isotherm plots of styrofoam waste-derived activated carbon

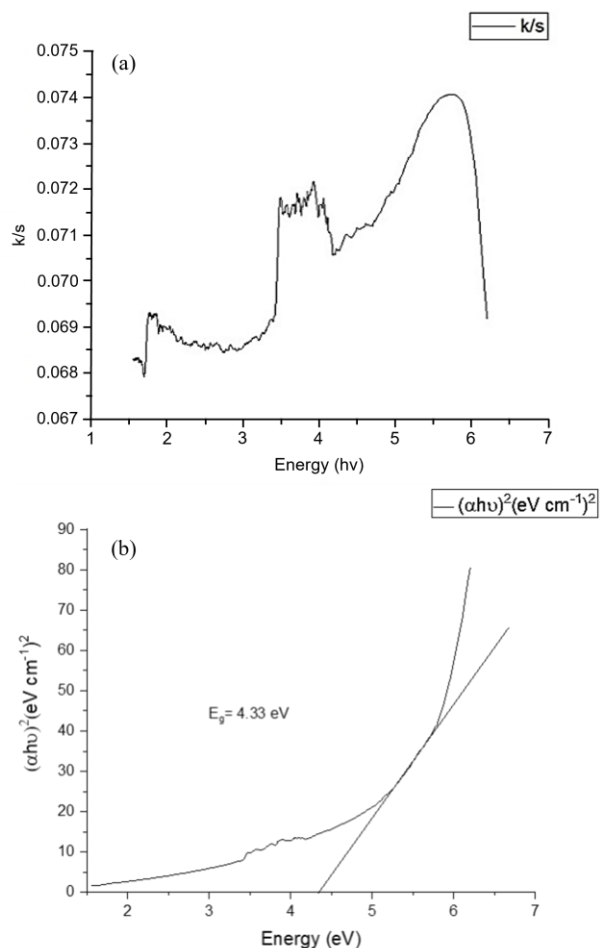


Figure 3. UV-DRS results of the Kubelka-Munk method for styrofoam waste-derived activated carbon: (a) graph of the Kubelka-Munk relationship to energy, (b) direct band gap energy derived from the Kubelka-Munk method

The graph in Figure 3 shows that the direct band gap energy of styrofoam waste-derived activated carbon is 4.33 eV, which falls within the semiconductor range of 0 eV < E_g < 5 eV [8], indicating that the activated carbon is a semiconductor. Other activated carbons, such as those derived from andiroba shells, have also been reported as semiconductors [23]. The band gap energy influences the ability of styrofoam waste-activated carbon to absorb light at longer wavelengths or lower energies. A smaller band gap energy allows for more effective light absorption, as it requires less energy to excite electrons from the valence band to the conduction band [15].

The band gap of styrofoam waste-derived activated carbon is relatively larger compared to other activated carbons, such as almond shell activated carbon, which has a band gap of 3.10 eV [24], and bamboo-activated carbon, which has a band gap of 3.3 eV [25]. The slightly wider band gap in styrofoam waste-derived activated carbon can help suppress the charge recombination process in photovoltaic cells by creating a greater separation between photogenerated electrons and holes [7].

Table 2. Light intensity measurements for photovoltaic cells

Activated carbon variation	Light intensity (lux)
F0	167,600
F1	169,300
F2	168,100
F3	169,800
F4	171,500
F5	170,900

3.2. Preparation of Cu/p-CuSCN/n-Cu₂O/Activated Carbon/ITO Photovoltaic Cells

Photovoltaic cells were successfully assembled by soaking the Cu plate in KSCN and acetic acid to form a CuSCN layer, followed by boiling in CuSO₄ to form a Cu₂O layer. Styrofoam waste-derived activated carbon was then deposited in varying amounts: F₀ (0 mg), F₁ (1 mg), F₂ (2 mg), F₃ (3 mg), F₄ (4 mg), and F₅ (5 mg), followed by the addition of ITO glass. The resulting photovoltaic cells exhibited a light blue top layer composed of Cu₂O, with activated carbon on top, as shown in Figure 4(a). The layer structure of the photovoltaic cells is depicted in Figure 4(b), with the layers arranged as follows: ITO glass, activated carbon, Cu₂O, CuSCN, and Cu. This cell configuration was developed based on the work of Karunarathna *et al.* [13], with modifications to the activated carbon layer.

3.3. Photovoltaic Cell Voltage Testing

The voltage test on the photovoltaic cells was conducted between 12:00 and 13:00 WIB under bright sunlight conditions, with light intensity ranging from 167,600 to 171,500 lux, as measured using a lux meter. The measurement data are presented in Table 2. The test was performed in triplicate, with the highest voltage obtained from the F₅ variation (5 mg activated carbon), which reached 209.67 mV. In contrast, the F₀ variation (without activated carbon) yielded only 73.33 mV. The voltage increase for the F₅ variation photovoltaic cell was significant, with a rise of 185.92% compared to F₀, as shown in Figure 5.

The detailed test results show that the F₀ photovoltaic cell produced a voltage of 73.33 mV, F₁ produced 95.67 mV, F₂ produced 129 mV, F₃ produced 136.33 mV, F₄ produced 162.33 mV, and F₅ produced 209.67 mV. CuSCN, a hole transport material, has a high conduction band value, which enhances hole collection efficiency and prevents recombination between electrons and holes [26]. The properties of CuSCN contribute to high efficiency in photovoltaic cells, minimizing energy loss through recombination. The combination of activated carbon and CuSCN in photovoltaic cells shows promising potential, as it improves electron and hole extraction by shortening the charge transport path. Moreover, the use of CuSCN and carbon leads to an energy shift of 0.2 eV [27], allowing for maximum photon absorption and higher voltages.

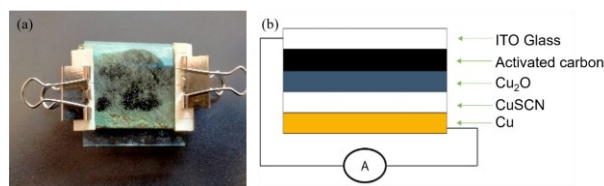


Figure 4. (a) photovoltaic cell plate and (b) layer structure of the photovoltaic cell

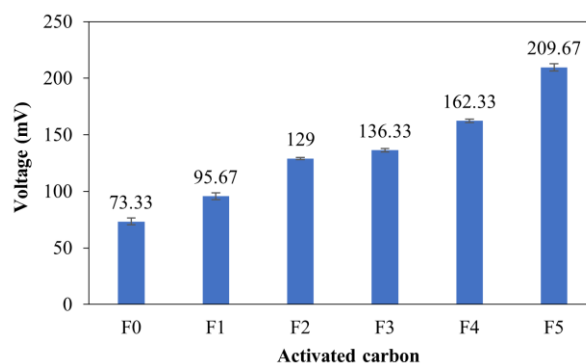


Figure 5. Voltage testing results of photovoltaic cells

The increase in voltage observed with the addition of activated carbon mass is also influenced by the pore size of the activated carbon, which is sufficiently large to accommodate n-Cu₂O within its pores, thereby facilitating the extraction of photogenerated electrons [13]. The incorporation of carbon materials, such as activated carbon, into photovoltaic cells can also enhance their longevity. This is due to the hydrophobic nature of carbon, which helps prevent degradation from humidity, thus improving the stability of the photovoltaic cells [28]. These findings suggest that activated carbon can serve as a cost-effective alternative to expand the electrode surface area and enhance the stability of photovoltaic cells, making it a viable option for large-scale production compared to conventional electrode materials.

4. Conclusion

Styrofoam waste-derived activated carbon exhibits excellent pore characteristics, with a surface area of 1,865.04 m²g⁻¹, a pore volume of 1.25 cm³g⁻¹, and an average pore diameter of 2.68 nm, classifying it as mesoporous. The mesoporous structure offers the advantage of maximizing light absorption across a wide range of wavelengths while being small enough to prevent the diffusion of captured electrons. When applied to Cu/p-CuSCN/n-Cu₂O/ITO-based photovoltaic cells,

activated carbon significantly enhances the voltage output, demonstrating its effectiveness as an electron extractor. The highest voltage, 209.67 mV, was achieved with the variation containing 5 mg of activated carbon (F5). Additionally, the direct band gap energy of styrofoam waste-derived activated carbon is 4.33 eV.

Acknowledgment

We would like to express our sincere gratitude to the Directorate of Learning and Student Affairs, Directorate General of Higher Education, Research, and Technology – Ministry of Education, Culture, Research, and Technology for their funding support of the *Program Kreativitas Mahasiswa Riset Eksakta* (PKM RE) tahun 2023. We also extend our thanks to Diponegoro University for their additional funding and facilitation in the successful implementation of the PKM activities.

References

- [1] World Population Review, *Plastic Pollution by Country*, 2016
- [2] M. M. Harussani, S. M. Sapuan, Umer Rashid, A. Khalina, R. A. Ilyas, Pyrolysis of polypropylene plastic waste into carbonaceous char: Priority of plastic waste management amidst COVID-19 pandemic, *Science of The Total Environment*, 803, (2022), 149911 <https://doi.org/10.1016/j.scitotenv.2021.149911>
- [3] Mohamed E. Mahmoud, Azza E. H. Abdou, Somia B. Ahmed, Conversion of Waste Styrofoam into Engineered Adsorbents for Efficient Removal of Cadmium, Lead and Mercury from Water, *ACS Sustainable Chemistry & Engineering*, 4, 3, (2016), 819-827 <https://doi.org/10.1021/acssuschemeng.5b01149>
- [4] Kartika Udyani, Erlinda Ningsih, Ambarwati Syahdiana Umar, Pengolahan Sampah Plastik Kemasan Minyak Goreng dan Tutup Botol menjadi Karbon Aktif, *Prosiding SENASTITAN: Seminar Nasional Teknologi Industri Berkelanjutan*, 2021
- [5] Alimuddin Muchtar, Analisis Emisi CO₂ PLTP Ulubelu Lampung dan Kotribusinya Terhadap Pengembangan Pembangkit Listrik di Provinsi Lampung, *Jurnal Pengelolaan Sumberdaya Alam dan Lingkungan (Journal of Natural Resources and Environmental Management)*, 9, 2, (2019), 288-303 <https://doi.org/10.29244/jpsl.9.2.288-303>
- [6] Xinzheng Lan, Silvia Masala, Edward H. Sargent, Charge-extraction strategies for colloidal quantum dot photovoltaics, *Nature Materials*, 13, 3, (2014), 233-240 <https://doi.org/10.1038/nmat3816>
- [7] Jarosław Serafin, Mohammed Ouzzine, Congcong Xing, Hajar El Ouahabi, Adrianna Kamińska, Joanna Sreńscek-Nazzal, Activated carbons from the Amazonian biomass andiroba shells applied as a CO₂ adsorbent and a cheap semiconductor material, *Journal of CO₂ Utilization*, 62, (2022), 102071 <https://doi.org/10.1016/j.jcou.2022.102071>
- [8] Sangtae Kim, Miso Lee, Changho Hong, Youngchae Yoon, Hyungmin An, Dongheon Lee, Wonseok Jeong, Dongsun Yoo, Youngho Kang, Yong Youn, Seungwu Han, A band-gap database for semiconducting inorganic materials calculated with hybrid functional, *Scientific Data*, 7, (2020), 387 <https://doi.org/10.1038/s41597-020-00723-8>
- [9] Lela Mukmilah Yuningsih, Dikdik Mulyadi, Pengaruh Aktivasi Karbon Aktif dari Tongkol Jagung dan Tempurung terhadap Nilai Konduktifitas, *Jurnal SANTIKA : Jurnal Ilmiah Sains dan Teknologi*, 6, 2, (2016), 531-536
- [10] Jun Liu, Michael Durstock, Liming Dai, Graphene oxide derivatives as hole- and electron-extraction layers for high-performance polymer solar cells, *Energy & Environmental Science*, 7, 4, (2014), 1297-1306 <https://doi.org/10.1039/C3EE42963F>
- [11] A. R. Hidayu, N. F. Mohamad, S. Matali, A. S. A. K. Sharifah, Characterization of Activated Carbon Prepared from Oil Palm Empty Fruit Bunch Using BET and FT-IR Techniques, *Procedia Engineering*, 68, (2013), 379-384 <https://doi.org/10.1016/j.proeng.2013.12.195>
- [12] L. Stobinski, B. Lesiak, A. Malolepszy, M. Mazurkiewicz, B. Mierzwa, J. Zemek, P. Jiricek, I. Bieloshapka, Graphene oxide and reduced graphene oxide studied by the XRD, TEM and electron spectroscopy methods, *Journal of Electron Spectroscopy and Related Phenomena*, 195, (2014), 145-154 <https://doi.org/10.1016/j.elspec.2014.07.003>
- [13] P. G. D. C. K. Karunarathna, C. A. N. Fernando, S. N. T. De Silva, Photocurrent Enhancement of Cu/p-CuSCN/n-Cu₂O Quantum Dot (QD) Novel Solid State Photovoltaic Cell with Coconut Shell Activated Carbon (CAC) as the Upper Electrode, *Journal of Scientific and Technical Research*, 6, 2, (2016),
- [14] Fabiano G. F. de Paula, Mateus C. M. de Castro, Paulo F. R. Ortega, Clara Blanco, Rodrigo L. Lavall, Ricardo Santamaria, High value activated carbons from waste polystyrene foams, *Microporous and Mesoporous Materials*, 267, (2018), 181-184 <https://doi.org/10.1016/j.micromeso.2018.03.027>
- [15] P. G. D. C. K. Karunarathna, S. P. A. U. K. Samarakoon, C. A. N. Fernando, Explanation of the photocurrent generation of Cu₂O quantum dots (QDs) sensitized p-CuSCN stable photoelectrochemical cells, *Materials Research Express*, 5, (2018), 015005 <https://doi.org/10.1088/2053-1591/aa9aa8>
- [16] Syarwan Hamid, Andi Aladin, Basri Modding, Takdir Syarif, Lastri Wiyani, Muh Arman, Pengaruh Aliran Nitrogen Kontinyu ke Dalam Reaktor Pirolisis Limbah Biomassa Serbuk Gergaji Batang Kelapa (*Cocos Nucifera*) Terhadap Nilai Kalor, *Journal of Chemical Process Engineering*, 8, 1, (2023), 1-6
- [17] S. Pérez-Huertas, M. Calero, A. Ligeró, A. Pérez, K. Terpiłowski, M. A. Martín-Lara, On the use of plastic precursors for preparation of activated carbons and their evaluation in CO₂ capture for biogas upgrading: a review, *Waste Management*, 161, (2023), 116-141 <https://doi.org/10.1016/j.wasman.2023.02.022>
- [18] Ulrike Ciesla, Ferdi Schüth, Ordered mesoporous materials, *Microporous and Mesoporous Materials*, 27, 2, (1999), 131-149 [https://doi.org/10.1016/S1387-1811\(98\)00249-2](https://doi.org/10.1016/S1387-1811(98)00249-2)
- [19] Jasmininder Singh, Soumen Basu, Haripada Bhunia, Dynamic CO₂ adsorption on activated carbon adsorbents synthesized from polyacrylonitrile (PAN): Kinetic and isotherm studies, *Microporous*

- and *Mesoporous Materials*, 280, (2019), 357-366
<https://doi.org/10.1016/j.micromeso.2019.02.031>
- [20] Chao Ge, Jian Song, Zhangfeng Qin, Jianguo Wang, Weibin Fan, Polyurethane Foam-Based Ultramicroporous Carbons for CO₂ Capture, *ACS Applied Materials & Interfaces*, 8, 29, (2016), 18849-18859 <https://doi.org/10.1021/acsami.6b04771>
- [21] Noemi Linares, Ana M. Silvestre-Albero, Elena Serrano, Joaquín Silvestre-Albero, Javier García-Martínez, Mesoporous materials for clean energy technologies, *Chemical Society Reviews*, 43, 22, (2014), 7681-7717
<https://doi.org/10.1039/c3cs60435g>
- [22] Salmon Landi, Iran Rocha Segundo, Elisabete Freitas, Mikhail Vasilevskiy, Joaquim Carneiro, Carlos José Tavares, Use and misuse of the Kubelka-Munk function to obtain the band gap energy from diffuse reflectance measurements, *Solid State Communications*, 341, (2022), 114573
<https://doi.org/10.1016/j.ssc.2021.114573>
- [23] M. K. Halimah, W. H. Chiew, H. A. A. Sidek, W. M. Daud, Z. A. Wahab, A. M. Khamirul, SM Iskandar, Optical properties of lithium borate glass (Li₂O)_x(B₂O₃), *Sains Malaysiana*, 43, 6, (2014), 899-902
- [24] S. K. Shahcheragh, M. M. Bagheri Mohagheghi, A. Shirpay, Effect of physical and chemical activation methods on the structure, optical absorbance, band gap and urbach energy of porous activated carbon, *SN Applied Sciences*, 5, 12, (2023), 313
<https://doi.org/10.1007/s42452-023-05559-6>
- [25] Luna Jena, Dhani Soren, Pratap Kumar Deheri, Puspallata Pattojoshi, Preparation, characterization and optical properties evaluations of bamboo charcoal, *Current Research in Green and Sustainable Chemistry*, 4, (2021), 100077
<https://doi.org/10.1016/j.crgsc.2021.100077>
- [26] Patrick Tonui, Saheed O. Oseni, Gaurav Sharma, Qingfenq Yan, Genene Tessema Mola, Perovskites photovoltaic solar cells: An overview of current status, *Renewable and Sustainable Energy Reviews*, 91, (2018), 1025-1044
<https://doi.org/10.1016/j.rser.2018.04.069>
- [27] Elang Barruna, Atya Saniah, Siti Fauziyah Rahman, Nji Raden Poespawati, Material Characteristics and Electrical Performance of Perovskite Solar Cells with Different Carbon-Based Electrodes Mixed with CuSCN, *Journal of Electrical and Computer Engineering*, 2023, 1, (2023), 8931693
<https://doi.org/10.1155/2023/8931693>
- [28] Rui He, Xiaozhou Huang, Mason Chee, Feng Hao, Pei Dong, Carbon-based perovskite solar cells: From single-junction to modules, *Carbon Energy*, 1, 1, (2019), 109-123 <https://doi.org/10.1002/cey2.11>